Supporting Material:

Sub-millisecond elastic recoil reveals molecular origins of fibrin fiber mechanics

Nathan E. Hudson, Feng Ding, Igal Bucay , E. Timothy O'Brien III, Oleg V. Gorkun, Richard Superfine , Susan T. Lord, Nikolay V. Dokholyan , Michael R. Falvo

Rouse Relaxation

The Rouse model for the relaxation time of an un-entangled polymer chain is given by $\tau_R \sim \eta b^3 N^2 / k_B T$ [1, 2], where η is the viscosity (0.001 Pa*s for water), b is the Kuhn length (~ 1 nm for a polypeptide), N is the number of connected segments of the Kuhn length (for a 300 amino acid chain, N~100 given each amino acid adds 0.34 nm of contour length) and $k_B T$ is the thermal energy at room temperature ($4.1*10^{-21}$ J). A 100 amino acid chain yields a 0.2 μs relaxation time, while a 300 amino acid chain yields 2.5μs.

Modeling the Elastic Recoil of the Fibrin Fibers.

We created a continuum mechanics model to represent the recoiling fibrin fiber moving through a viscous medium. Our goal was to obtain an estimate of recoil time and compare this estimate with our experimental results. We modeled the fiber in the fluid as spring-dashpot system, with the elastic properties of the fiber represented by the spring, and the viscous drag of the fluid on the fiber represented by the dashpot. The model parameters include the fiber elongation $x(t)$, the viscous drag coefficient γ, and effective spring constant k_{eff} . The equation of motion is given by:

$$m\ddot{x}(t) + \gamma\dot{x}(t) + k_{eff}\,x(t) = 0 \qquad \text{(S1)}$$

To make an estimate of fiber spring constant, we treated the fiber as consisting of protofibrils connected by αC domains in series and parallel, across and down the fiber. We recently developed a mechanical model for the fiber consisting of a network of entropic "worm-like" polymer chains (representing the αC connector regions) interconnected in parallel in series across the fiber [3]. This model predicts a whole-fiber spring constant given by:

$$keff = \left(\frac{N}{M}\right)\frac{k_B T}{L_c L_p} \qquad \text{(S2)}$$

Where N is the number of parallel connections, M is the number of series connections and L_c and L_p are the contour and persistence lengths respectively of the unstructured sections of the αC region. Persistence lengths for unfolded polypeptide chains have been measured in many force spectroscopy experiments and typically range of 0.3-1.0 nm. We use L_p=0.5nm in our model. The contour length depends on the number of amino acids in the unstructured portions of the αC region. In the model we use 400 amino acids (200 on each aC region) resulting in L_c=120nm (0.34 nm / amino acid). For the experimentally observed range of fiber diameters this yields a k_{eff} ~0.3 nN/μm – 4.8 nN/μm. As a comparison, one can make a continuum mechanics estimate of the effective spring constant of the fiber with the known Young's modulus and fiber geometry ($k_{eff} = E * A / L$, where E is the Young's modulus, A is the cross sectional area, and L is the fiber length). Experiments show fibrin fibers have a Young's modulus of 2-10MPa, and diameters of 50-300nm [4, 5]. In these experiments, the fiber has an initial length of 10μm. This yields a

range of spring constants from 0.9 nN/μm to 15 nN/μm, in reasonable agreement. For the fiber friction coefficient, we model the fiber as a cylinder moving through a viscous medium. The average friction coefficient is given by the Oseen treatment of viscous drag on a cylinder [6] at low Reynolds number:

$$\gamma = \frac{2\pi\eta L}{\ln(\frac{L}{2D})} \tag{S3}$$

Where η is the solvent viscosity (0.001 Pa*s at 20°C), and L and D are the length and diameter of the fiber respectively. This yields a cylinder drag coefficient of order 10^{-8} Ns/m.

To estimate the mass of the fiber, we take into account the number of molecules down the length and across the width of the fiber. For a 10μm long fiber, the number of molecules down the length is estimated as 10μm/45nm ~ 220. The number of molecules across the width of a fiber is approximated as the square of the ratio of the fiber diameter to the molecular diameter. The estimated mass of the fiber ranges from 10^{-18}-10^{-16} kg. The very small mass renders the first term in Eqn. S1 negligible (inertia is not relevant to the dynamics). Neglecting the first term and solving Eqn. 1 to obtain the fiber's equation of motion yields a simple decaying exponential with decay time constant given by:

$$\tau = \gamma / k_{eff} \tag{S4}$$

Given the estimated drag coefficient and range of spring constants, this yields a range of relaxation time constants of between 0.1-10ms. These theoretical results, which were not determined through any fitting to data, further support the elastomeric origins of fibrin fiber properties, and show that our experimentally observed recoil time is in agreement with a simple continuum mechanics treatment. It is likely that molecular scale models involving crowding and mechanisms of fiber tension will be needed to further explain this recoil behavior, especially the slower tensing time which this model does not capture.

Experimental Measurement as it Relates to Strain. As a consequence of the transverse fiber stretching method used in the study, the position data represent the transverse deflection of the center of the fiber along a coordinate axis perpendicular to the original fiber axis. This is the maximum deflection of the fiber from its relaxed position; we'll denote this time dependent parameter, *x(t)*. All curve fitting was performed on *x(t)* data determined from the raw ROI movie files that captured the center position of the fibers within each image. The resultant exponential decay time constants (τ_1 and τ_2) describe the exponential decay of *x(t)*. In tensile stretching/recoil contexts, tensile elongation, ΔL, or strain, $\varepsilon = \Delta L/L_0$, are the proper parameters to describe deformation and relaxation (where ΔL is the change in fiber length and L_0 is the relaxed length. See fig S1). Our experimental parameter *x(t)*, is a function of fiber strain $\varepsilon(t)$, but is not linearly related. Therefore the exponential decay time constants determined by fitting *x(t)* do not directly translate as a measure of the exponential decay in strain. However, the exponential decay constants for *x(t)* are related to those for strain in a simple way as we will show below. Although experimental necessity required measuring *x(t)* rather than $\varepsilon(t)$ directly, the geometrical "advantage" of the *x(t)* parameter is that it is a more sensitive measure of fiber recoil for small strain ($x(t) = (L_0+\Delta L)/\sin(\theta)$). At small strains, we can collect reliable *x(t)* data where direct strain measurements would have inherently higher experimental uncertainty. This benefited our exponential fits.

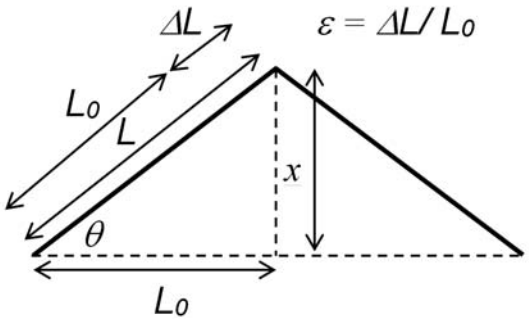

Figure S1. Schematic of fibrin stretching experiment and parameter definitions.

As shown for the over-damped harmonic oscillator model described above, we expect that the extended fiber will recoil to its relaxed length according to a decaying exponential with decay time constant τ. In the following calculations, we determine the time dependence of *x(t)* given our experimental geometry and the assumed decaying exponential time dependence of strain, ε (or equivalently extension, ΔL).

$$L(t) - L_0 = \Delta L(t) = \Delta L_{\max} e^{-\frac{t}{\tau}} \tag{S5}$$

Substitute

$$\Delta L_{\max} = \varepsilon_{\max} L_0 \quad ; \quad \Delta L(t) = \sqrt{L_0^2 + x(t)^2} - L_0 \tag{S6, S7}$$

$$\sqrt{L_0^2 + x(t)^2} - L_0 = \varepsilon_{\max} L_0 e^{-\frac{t}{\tau}} \tag{S8}$$

$$\sqrt{L_0^2 + x(t)^2} = L_0(\varepsilon_{\max} e^{-\frac{t}{\tau}} + 1) \tag{S9}$$

$$L_0^2 + x(t)^2 = L_0^2(\varepsilon_{\max}^2 e^{-\frac{2t}{\tau}} + 2\varepsilon_{\max} e^{-\frac{t}{\tau}} + 1) \tag{S10}$$

$$x(t)^2 = L_0^2 \varepsilon_{\max}^2 e^{-\frac{2t}{\tau}} + 2\varepsilon_{\max} L_0^2 e^{-\frac{t}{\tau}} \tag{S11}$$

$$x(t)^2 = L_0^2 \varepsilon_{\max} e^{-\frac{t}{\tau}} (\varepsilon_{\max} e^{-\frac{t}{\tau}} + 2) \tag{S12}$$

$$x(t) = L_0 \varepsilon_{\max}^{1/2} e^{-\frac{t}{2\tau}} (\varepsilon_{\max} e^{-\frac{t}{\tau}} + 2)^{1/2} \tag{S13}$$

The term on the right side of Eqn. S13 within the parenthesis has a very weak time dependence over all time scales as compared to the factor that precedes it. It will vary from $(\varepsilon_{\max} + 2)^{1/2}$ to $2^{1/2}$ over the

whole decay. For a maximum strain of 1.0 , this factor will vary only 20% over the whole time range *t=0* to *t=infinity*. Given that *x(t)* varies over many orders of magnitude, this factor's time dependence is insignificant and can be approximated as a constant. Since we are only interested in the time dependence of *x(t)* for the purposes of fitting a decaying exponential, we wrap all constants into a single prefactor x_{max}:

$$x(t) = x_{\max} e^{-\frac{t}{2\tau}} \tag{S14}$$

This indicates that the exponential decay constant found by fitting our *x(t)* data is approximately twice the value of the exponential decay constant describing the strain or extension of the fiber.

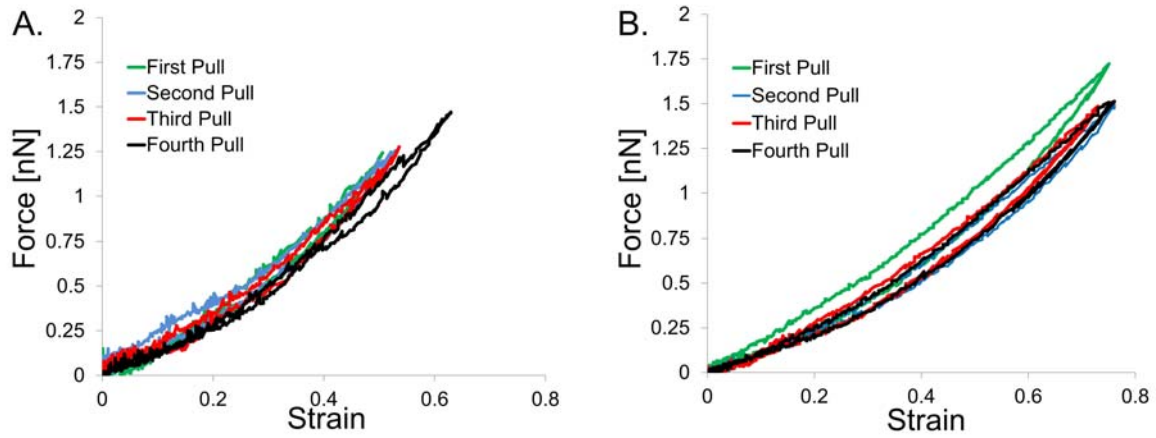

Figure S2. Mechanical Reversibility of Fiber Strain. The plots depict typical force vs. strain data taken on both un-ligated and FXIIIa ligated fibrin fibers that verify fibrin fibers' high elasticity. In each case the fiber was stretched 4 times, with each entire stretch cycle taking 11s. **A,** For the un-ligated fiber, no significant change in the force vs. strain is apparent. For the ligated fiber in **B,** there is a slight difference between the first and subsequent curves. The effective change in stiffness in this particular case is less than 10% between the first and second pull, and then for the 2nd through 4th pull, no change is apparent. This typical behavior in that we did not see changes in stiffness of more than 10% over the course of several pulls

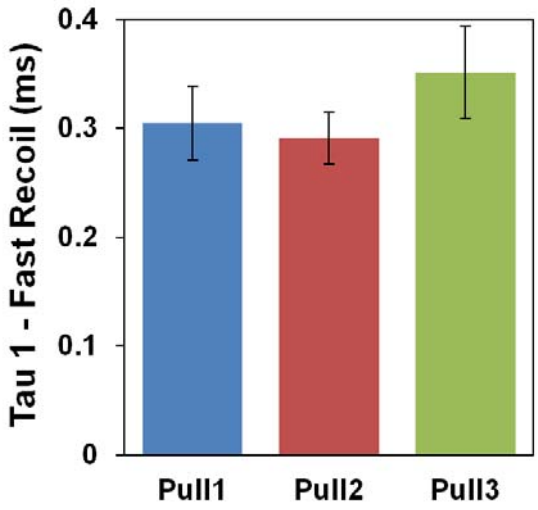

Figure S3. Fast Recoil Time (τ_1) Is Reproducible Over Several Pulls. There was no significant change in the fast recoil time over three pulls. 20 fibers were measured. ($P > 0.1$ for all comparisons; Error bars indicate SEM).

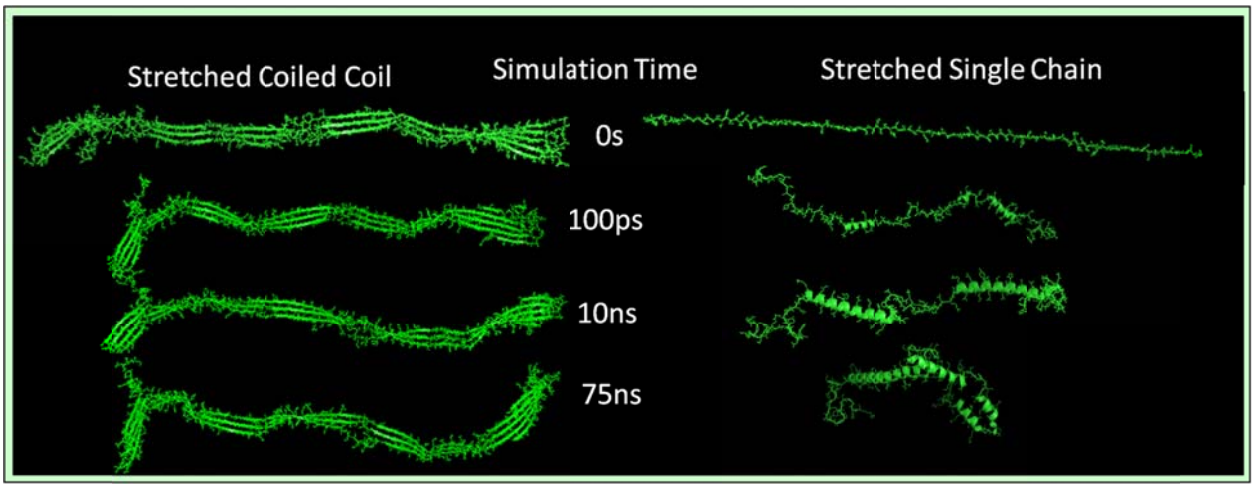

Figure S4. β-sheet Relaxation: Left: Simulations of the β-sheet form of the stretched fibrin coiled-coil. The β-sheet form is obtained by stretching the coiled-coil at constant force. Once formed, the β-sheet contacts were stable within our simulation timescales, and prevented recoil. Right: Simulations of the γ chain of the coiled coil part of the molecule. Contrary to the β-sheet case on the left, the γ chain in isolation immediately collapses and begins re-forming an α-helix structure. The collapse happens faster than would be expected in the real system due to the use of an implicit solvent (no explicit viscous drag).

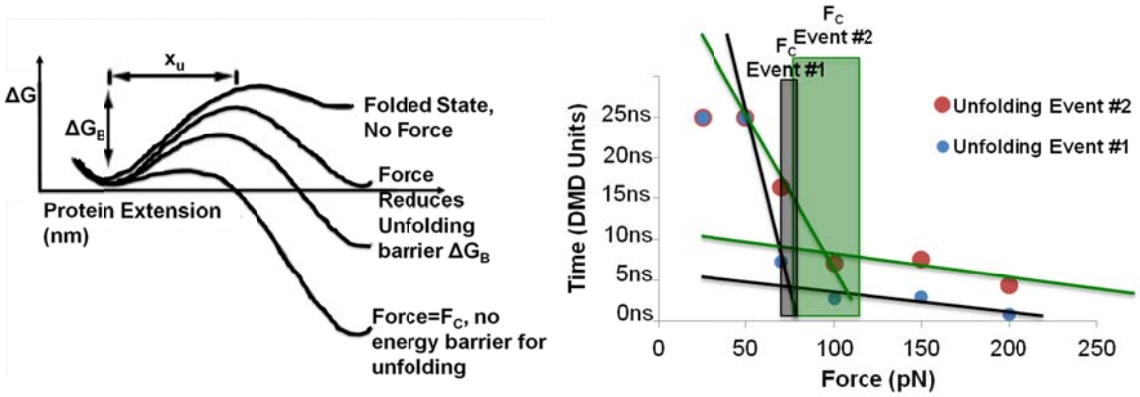

Figure S5: Forced Unfolding of the γ-C domain: The image on the left represents the unfolding energy landscape for a protein. The energy barrier height can be effectively reduced through the application of force. At the critical force (F_C), the unfolding barrier is eliminated leading to unfolding. Right. These data were used to estimate the F_C for the two unfolding events of the γ-nodule. The unfolding time for events #1 and #2 is plotted as a function of applied force. The grey and green shaded areas represent the uncertainty range of the estimated force for event #1 (74±7pN) and event #2 (89±21pN) respectively.

MOVIE CAPTIONS:

Movie S1: Full Frame Fibrin Fiber Recoil: Movie of the relaxation of a fibrin fiber. The movie was taken at 300 frames per second. Within one frame the fiber regains 85% of its strain, and over the next 4ms, it regains its initial length.

Movie S2: Region of Interest (ROI) Fibrin Fiber Recoil: Movie taken at 4000 frames per second centered on the middle of the fiber. Capturing at higher frame rates allowed the fast and slow recoil time constants to be measured.

Movie S3: Coiled Coil Stretching: Simulations pulling at constant force on the coiled coil region of the molecule indicate an alpha-helix to beta-sheet transition during stretching. This representative movie shows a 5ns simulation at a constant force at 700pN. The alpha-helix to beta-sheet transition occurs simultaneously with the stretching of the molecule. Similar behavior was observed at all forces simulated above the critical force, although the unfolding time scales exponentially with force.

Movie S4: γ-Nodule Stretching: The γ-nodule was stretched at constant force and displayed a sequential unfolding. Force was applied at the end of the synthetic knob peptide mimic. In this representative simulation, the applied force is 200pN. Stretching at the knob:hole interface induced a sequential unfolding of the γ-nodule with distinct critical unfolding forces. As expected from their determined critical forces, the coiled-coil region remains folded as the γ-nodule unfolds. This highlights the difference in their relative stabilities under force.

SUPPORTING REFERENCES:

1. Rubinstein, M. and R.H. Colby, *Polymer Physics*. 2003, Oxford, UK: Oxford University Press.
2. Rouse, P.E., *A Theory of the Linear Viscoelastic Properties of Dilule Solutions of Coiling Polymers.* J. Chem. Phys., 1953. **21**(7): p. 9.
3. Houser, J.R., N.E. Hudson, L. Ping, E.T. O'Brien, 3rd, R. Superfine, S.T. Lord, and M.R. Falvo, *Evidence that alphaC region is origin of low modulus, high extensibility, and strain stiffening in fibrin fibers.* Biophys J, 2010. **99**(9): p. 3038-47.
4. Collet, J.P., H. Shuman, R.E. Ledger, S. Lee, and J.W. Weisel, *The elasticity of an individual fibrin fiber in a clot.* Proc Natl Acad Sci U S A, 2005. **102**(26): p. 9133-7.
5. Weisel, J.W., C. Nagaswami, and L. Makowski, *Twisting of fibrin fibers limits their radial growth.* Proc Natl Acad Sci U S A, 1987. **84**(24): p. 8991-5.
6. Venier, P., A.C. Maggs, M.-F. Carlier, and D. Pantaloni, *Analysis of microtubule rigidity using hydrodynamic flow and thermal fluctuations.* J. Biol. Chem, 1994. **269**(18): p. 13353 - 13360.